Environmental Science and Ecotechnology 22 (2024) 100477

Contents lists available at ScienceDirect

Environmental Science and Ecotechnology

journal homepage: www.journals.elsevier.com/environmental-science-and-ecotechnology/

Original Research

Wintertime ozone surges: The critical role of alkene ozonolysis

Jin Yang [a, 1], Yangzong Zeren [a, b, 1], Hai Guo [a, b, *], Yu Wang [a, b, **], Xiaopu Lyu [c], Beining Zhou [a], Hong Gao [d], Dawen Yao [a], Zhanxiang Wang [d], Shizhen Zhao [e], Jun Li [e], Gan Zhang [e]

[a] Air Quality Studies, Department of Civil and Environmental Engineering, Kowloon, 999077, The Hong Kong Polytechnic University, Hong Kong, China
[b] Research Institute for Land and Space, The Hong Kong Polytechnic University, Kowloon, 999077, Hong Kong, China
[c] Department of Geography & Smart Society Lab, Hong Kong Baptist University, Kowloon, 999077, Hong Kong, China
[d] Key Laboratory for Environmental Pollution Prediction and Control, College of Earth and Environmental Sciences, Lanzhou University, Lanzhou, Gansu, 730050, China
[e] Guangzhou Institute of Geochemistry, Chinese Academy of Sciences, Guangzhou, 511443, China

ARTICLE INFO

Article history:
Received 16 February 2024
Received in revised form
13 August 2024
Accepted 14 August 2024

Keywords:
Ozone pollution
Winter
Alkenes
Radical chemistry
PBM-MCM

ABSTRACT

Ozone (O_3) pollution is usually linked to warm weather and strong solar radiation, making it uncommon in cold winters. However, an unusual occurrence of four high O_3 episode days (with maximum hourly concentrations exceeding 100 ppbv and peaking at 121 ppbv) was recorded in January 2018 in Lanzhou city, China. During these episodes, the average daytime concentration of total non-methane volatile organic compounds (TVOCs) reached 153.4 ± 19.0 ppbv, with alkenes—largely emitted from the local petrochemical industry—comprising 82.3 ± 13.1 ppbv. Here we show a photochemical box model coupled with a Master Chemical Mechanism to elucidate the mechanisms behind this unusual wintertime O_3 pollution. We find that the typically low temperatures (−1.7 ± 1.3 °C) and weak solar radiation (263.6 ± 60.7 W m^{-2}) of those winter episode days had a minimal effect on the reactivity of VOCs with OH radicals. Instead, the ozonolysis of alkenes generated Criegee intermediates, which rapidly decomposed into substantial RO_x radicals (OH, HO_2, and RO_2) without sunlight. This radical production led to the oxidation of VOCs, with alkene ozonolysis ultimately contributing to 89.6 ± 8.7% of the O_3 formation during these episodes. This mechanism did not activate at night due to the depletion of O_3 by the NO titration effect. Furthermore, the findings indicate that a reduction of alkenes by 28.6% or NO_x by 27.7% in the early afternoon could significantly mitigate wintertime O_3 pollution. Overall, this study unravels the unique mechanism of alkene-induced winter O_3 pollution and offers a reference for winter O_3 reduction strategies in the petrochemical industrial regions.

1. Introduction

Ground-level ozone (O_3) pollution has attracted public attention in the past decades due to its detrimental impacts on human health, vegetation growth, and climate change [1–5]. Tropospheric O_3 concentrations are influenced by photochemical reactions among O_3 precursors (i.e., nitrogen oxides [NO_x = NO + NO_2], volatile organic compounds [VOCs], and carbon monoxide [CO]), as well as by regional transport and stratosphere–troposphere exchange [6–9]. In addition to the concentrations of O_3 precursors, the chemical formation of O_3 is highly related to meteorological conditions (i.e., temperature and solar radiation). High temperatures and strong solar radiation are conducive to the chemical production of O_3 [10–16]. As such, O_3 pollution events are generally concentrated in spring, summer, and autumn but rare in winter [17–20]. However, a handful of studies have reported O_3 episode events (maximum hourly concentration exceeding 100 ppbv) in winter at specific locations with high surface albedo values and/or heavy precursor emissions [21–24]. For example, in the winter of 1993, hourly O_3 peaks of 100–120 ppbv were discovered in Delhi,

* Corresponding author. Air Quality Studies, Department of Civil and Environmental Engineering, Kowloon, 999077, China.
** Corresponding author. Air Quality Studies, Department of Civil and Environmental Engineering, Kowloon, 999077, China.
E-mail addresses: ceguohai@polyu.edu.hk (H. Guo), yu.6.wang@polyu.edu.hk (Y. Wang).
[1] These authors contributed equally to this work.

https://doi.org/10.1016/j.ese.2024.100477

India, due to meteorological conditions favorable to the accumulation of air pollutants [21]. In addition, in February 2008, O_3 pollution events occurred in a natural gas field in Wyoming, the United States of America (USA) (hourly maximum value attaining 140 ppbv) with a daily average temperature of −17 °C. These were attributed to high concentrations of O_3 precursors (i.e., alkanes) trapped by the shallow temperature inversion [22]. Moreover, in 2013, due to high snow albedo and strong carbonyl photolysis, severe O_3 pollution was found in the oil fields of Utah, USA, with a daily average temperature being −8 °C [23,24].

In China, surprisingly, high O_3 values during cold weather have been widely observed in North China in recent years (Supplementary Material Fig. S1). On the one hand, the reduction in NO_x emissions since 2013 has resulted in enhanced O_3 pollution in the North China Plain [25]. On the other hand, large O_3 precursor emissions from oil fields and/or petrochemical industrial areas have led to intensive production of O_3 in winter [22–24,26,27]. Specifically, several high O_3 days (maximum hourly values around 80 ppbv) in winter were observed in oil fields in the Yellow River Delta (YelRD) region, which were ascribed to heavy emissions of alkanes during oil extraction operations [28]. In addition, highly reactive VOCs (i.e., ethene, propene, toluene, and xylene) emitted from industry sources, combined with favorable meteorological conditions for the accumulation of air pollutants, led to O_3 pollution (hourly maximum reaching 76 ppbv) in Shijiazhuang city in North China during the winter [29]. Moreover, it is notable that the highest O_3 concentration was discovered in Lanzhou during winter (Supplementary Material Fig. S1a and Table S1), which also experienced the highest frequency of days with high O_3 levels (Supplementary Material Fig. S1b). However, the driving factors of this unique O_3 episode event have not yet been explored.

Lanzhou is a typical industrial city in northwestern China, where the first discovery of photochemical smog dates back to the mid-1970s [30–32]. Apart from the dense air pollutants emitted from the local petrochemical industry [33–36], Lanzhou's basin topography contributes to poor air quality by creating unfavorable conditions for the diffusion of air pollutants [37,38]. Previous research on O_3 pollution in Lanzhou has mainly focused on the relationships between O_3 and its precursors. For example, it was found that the O_3 formation regime at an industrial site in Lanzhou transferred from a NO_x-limited regime to a transitional one in the summer [37–40]. In addition, the contributions of VOCs to O_3 production have been quantified [37,38,40]. Specifically, alkenes, especially C_4 alkenes emitted from the petrochemical industry, were identified as the most important contributors to O_3 formation [38,41]. However, these studies solely focused on O_3 formation in the summer, mainly due to the frequent occurrence of high O_3 days under intense solar radiation and high temperatures. On the contrary, the O_3 formation mechanisms in winter have seldom been reported. Therefore, the underlying causes of the extremely high O_3 concentrations observed in cold weather and times of weak solar radiation are worth exploring during wintertime. Furthermore, there is a lack of detailed information about the O_3 formation mechanisms, such as the evolution of O_3 precursors during photochemical reactions and their impacts on radical chemistry.

To fill these knowledge gaps, an intensive sampling campaign of O_3, its precursors, and meteorological parameters was conducted in Lanzhou during the winter of 2018. A photochemical box model incorporating a Master Chemical Mechanism (PBM-MCM) was employed to investigate the relationship between O_3 and weather conditions. More importantly, critical photochemical reactions were studied, including the evolution of VOCs and their contributions to O_3 production. Based on the results, emission control suggestions have been devised for O_3 mitigation in Lanzhou. The findings of this study will draw public attention to winter O_3 pollution and provide new insights into photochemistry with intensive alkene emissions.

2. Materials and methods

2.1. Sampling site and data collection

Lanzhou is one of the largest petrochemical bases in western China. The sampling site (36°06′ N, 103°37′ E, 1,695 m above sea level) was set up on the roof of the Lanyuan Hotel, which is located in a residential area affiliated with the PetroChina Lanzhou Petrochemical Company. It is 0.7 km and 2.2 km away from the industrial area and the highway, respectively (Supplementary Material Fig. S2). Basically, the sampling site receives the emissions originating from not only residents but also industrial and vehicle sources. A detailed description of the sampling site can be found in Text S1 (Supplementary Material).

Intensive sampling was conducted from January 1 to 31, 2018 (Supplementary Material Text S1). The hourly mixing ratios of O_3, NO, NO_2, CO, and SO_2 were recorded at the national monitoring site (https://www.cnemc.cn/, the same location as our sampling site). An online gas chromatograph−mass spectrometer was deployed to measure the concentrations of 60 VOC species: 29 alkanes, 16 aromatics, 14 alkenes, and one alkyne (Supplementary Material Table S2). Detailed information on the instrument type, measurement technique, detection limits, and time resolutions is listed in Table S3 (Supplementary Material). Oxygenated VOCs (OVOCs) were collected using silica cartridges impregnated with acidified 2,4-dinitrophenylhydrazine. After sampling, high-performance liquid chromatography was applied to determine the concentrations of 16 OVOCs (Supplementary Material Table S4). The sample collection, data quality assurance, and calibration methods are described in Text S2 (Supplementary Material). An autonomous weather station was operated at the sampling site to monitor meteorological parameters, including relative humidity, temperature, solar radiation, wind speed, and wind direction.

2.2. Photochemical box model

A PBM-MCM was used to reproduce O_3 photochemistry and determine the impacts of meteorological conditions on the reaction rates of O_3 precursors. The MCM (v3.3.1) details approximately 17,000 reactions and 6,600 intermediate species and well describes homogeneous gas-phase reactions in the atmosphere [42–45]. In addition, other parameters, such as the photolysis rate, dry deposition rate, development of the boundary layer, and aloft exchange are considered in this model. The coordinates of the sampling site and the observed solar radiation were also inputted into the model to calculate the photolysis rates through the tropospheric ultraviolet and visible radiation module [15,46–49]. The model has been applied to many cities in China, and its good performance in *in situ* photochemistry simulations has been widely proven [15,46–49].

The temperature, relative humidity, O_3, NO, NO_2, CO, SO_2, VOCs, and OVOCs data acquired at the sampling site in January 2018 were averagely interpolated into datasets with a time resolution of 600 s, and these were subsequently inputted into the model to simulate the O_3 formation mechanisms. The VOC and OVOC species applied in the model are marked in Tables S2 and S4 (Supplementary Materials). The concentrations of the other species listed in these tables were below the detection limits. The average diurnal profiles of nitrous acid (HONO) measured in previous studies were applied due to the lack of HONO observations (Supplementary Material Text S3) [50–53], and the uncertainties associated with HONO were quantitatively analyzed (Supplementary Material Fig. S3). In this study, we discovered that the radical concentrations would reach

statistical equilibrium within 18 h (Supplementary Material Fig. S4). Therefore, one−day preceding the study period was set as the model spin-up time to ensure the statistical equilibrium of the simulated results. The model validation method and results are shown in Texts S4−S5 and Fig. S5 (Supplementary Material), respectively, and the calculation formulas for reaction rates of formation/destruction pathways are described in Text S6 (Supplementary Material). The relative incremental reactivity (RIR) values were defined as the relative change in net O_3 production rate with variations of O_3 precursors [15,46,47,54,55]. These values were used to evaluate the sensitivity of O_3 production to its precursors. The detailed RIR calculations are in Text S7 (Supplementary Material). To qualify the uncertainties arising from the observed alkanes, alkenes, aromatics, OVOCs, and NO_x, sensitivity tests were performed through model simulations. The results are shown in Figs. S6−S10 (Supplementary Material), and the related analyses are discussed in Text S8 (Supplementary Material).

3. Results and discussion

3.1. Overview of O_3 pollution in winter

3.1.1. Winter O_3 pollution in China

Fig. S1a (Supplementary Material) presents the daily average maximum O_3 concentrations (> 80 ppbv) recorded in winter (defined as December, January, and February) at 1,590 monitoring stations in China during 2015−2020. Surprisingly, 76.3% of the monitoring stations (1,213 sites) recorded high concentrations of O_3, which sharply contrasts with the traditional understanding that O_3 pollution mainly occurs in the warmer season. Among these stations, 59.6% were in South China (crossed). The remaining 40.4% that witnessed high O_3 concentrations were located in North China (dotted), where the meteorological conditions were considered unfavorable for O_3 pollution (i.e., low temperatures and weak solar radiation). In addition, 37.0% of the stations (452 sites) recorded a frequency of O_3 pollution days (hourly O_3 concentration > 80 ppbv) of more than 1.0% during the winter days between 2015 and 2020 (Supplementary Material Fig. S1b). Analyzing the environment surrounding those sites revealed that rural sites were primarily near oil fields (gray-shaded areas) and that the urban sites were generally distributed in cities with petrochemical industries. Notably, Lanzhou experienced the highest frequency of O_3 pollution days (17.8%). Thus, Lanzhou is an ideal place to investigate the mechanisms underlying winter O_3 pollution.

3.1.2. Winter O_3 pollution in Lanzhou

Fig. S11 (Supplementary Material) shows a time series of the concentrations of trace gases and VOCs recorded in January 2018. Four O_3 episode days (January 1, 13, 16, and 20, shaded in red) were recorded, with an average daily maximum of 115.0 ± 8.5 ppbv, despite cold weather and weak solar radiation. The daytime average concentrations of NO and NO_2 were 16.0 ± 4.0 and 31.4 ± 3.4 ppbv, respectively, which were higher than those recorded in other cities in China [25,59−62], indicating a strong effect of NO titration. Furthermore, there were four more days (January 9−10, 12, and 23, shaded in blue) when the hourly maximum concentration of O_x (O_3 + NO_2) exceeded 100 ppbv. Overall, the O_3 pollution was severe in Lanzhou that winter, which may have resulted from local photochemical reactions due to high concentrations of O_x.

The concentrations of air pollutants and meteorological conditions recorded on O_3 episode days and non-episode days are compared in Fig. S12 (Supplementary Material). The average daytime temperature on O_3 episode days (−1.7 ± 1.3 °C) was higher than that on O_3 non-episode days (−5.7 ± 0.5 °C, *t*-test, $p < 0.05$), while the relative humidity on O_3 episode days was lower than that on O_3 non-episode days ($p < 0.05$) (Supplementary Material Table S5). The solar radiation, wind speed, and planetary boundary layer height (PBLH) levels were comparable ($p > 0.05$). Notably, concentrations of O_3 precursors, including CO, NO, NO_2, and total non-methane volatile organic compounds (TVOCs) were higher on O_3 episode days than on O_3 non-episode days ($p < 0.05$). In particular, the concentration of alkenes was almost 1.5 times that on O_3 non-episode days, and the diurnal pattern of alkene concentration showed an elevated concentration at 14:00 local time (LT) on O_3 episode days, which was significantly higher than that on O_3 non-episode days. However, no such difference was found in meteorological parameters. Thus, it can be speculated that the increase in the alkene concentration was related to local emissions. At relatively high temperatures and low relative humidity levels on O_3 episode days, the large amounts of O_3 precursors might have accelerated O_3 production [63−66].

In this study, the average daytime concentration of TVOCs on O_3 episode days was 153.4 ± 19.0 ppbv, which was considerably higher than that recorded at other industrial sites in China, such as Xi'an (85.3 ± 60.6 ppbv), Jiyuan (54.3 ± 27.5 ppbv), Wuhan (44.1 ppbv), Taiwan (64 ppbv), and Guanzhong Plain (42.4−74.3 ppbv) [67−71]. It was even comparable to that recorded at other oilfield sites around the world; for example, the YelRD region (171.2 ± 527.2 ppbv), Junggar Basin (213 ± 97.7 ppbv), Upper Green River Basin (230 ppbv), and Denver-Julesburg Basin (97 ppbv) [28,72−74]. Fig. S13a (Supplementary Material) shows the percentage of VOC groups and the average daytime concentrations of the top 20 VOC species on O_3 episode days. It is worth noting that alkenes (82.3 ± 13.1 ppbv) accounted for the largest proportion (53.7 ± 8.5%) of TVOCs, which was different from the results found in other oilfields where alkanes comprised the largest proportion (Supplementary Material Fig. S13b). Specifically, propene (35.2 ± 9.8 ppbv), ethene (25.1 ± 6.5 ppbv), and *trans*/*cis*-2-butene (7.8 ± 3.6 ppbv) accounted for the largest proportion of alkenes. Although the high reactivity of alkenes makes them suitable for involvement in strong photochemical reactions, the low temperatures and weak solar radiation levels of winter were not triggering factors for intensive O_3 production. Hence, the O_3 formation mechanism was elaborated in the following sections with the aid of PBM-MCM model simulations.

3.2. Influence of meteorological conditions on winter O_3 formation

We compared the meteorological conditions and air pollutant concentrations in winter and summer (Supplementary Material Table S5). The reduced PBLH in winter corresponded to higher levels of O_3 precursors than in summer. This might have resulted from weaker mixing and diffusion processes under the shallower PBLH in winter [56−58]. Notably, the relative humidity and temperature were much lower, and the solar radiation was weaker on the winter O_3 episode days compared to summer ones. Although previous studies have demonstrated that lower humidity leads to higher O_3 concentrations in the temperature range of 30 to −30 °C [65], the effects of temperature and solar radiation remain unclear. In Fig. S14 (Supplementary Material), panel a shows the effects of temperature on VOC reactivity with OH, while panel b displays the effect of solar radiation on simulated OH concentration. Weak solar radiation decreased the OH concentration, which could further inhibit O_3 formation. In contrast, an increase in temperature reduced the VOC reactivity of *trans*/*cis*-2-butene, while the VOC reactivity of 1,3,5-trimethylbenzene (135-TMB) was stable during temperature changes due to the value of the fixed constant *k* of 135-TMB and OH. Additionally, the reactivity of cyclohexane and OH slightly increased with increasing temperature.

To further investigate the impacts of temperature and solar radiation on O_3 formation, the reaction rates of alkanes, alkenes, and aromatics with OH were simulated under changes in temperature and solar radiation during the most active photochemical reaction period (13:00–16:00 LT, hereinafter the peak period) on O_3 episode days (Fig. 1a). The relationships between the reaction rates of VOCs and solar radiation were close to linear regressions, with slopes of 0.1, 2.0, and 0.1 ppbv h^{-1} per 100 W m^{-2} for alkanes, alkenes, and aromatics, respectively. In addition, the reaction rates of alkenes increased with increasing temperature below 10 °C and decreased slightly when the temperature exceeded 10 °C (Fig. 1b). The reaction rate of alkenes on winter O_3 episode days was only approximately 15% lower than that on summer O_3 episode days. It was lower than those of alkanes and aromatics (~30%). Upon further investigation of the alkene species, it was found that the reaction rate of *trans*/*cis*-2-butene increased slowly above 0 °C (Supplementary Material Fig. S14c). In general, low temperatures and weak solar radiation in winter reduced the reactivity of VOCs with OH to a certain extent but had a limited impact on the reaction rates of alkenes with OH.

3.3. Photochemical mechanisms underlying winter O_3 pollution

As shown in Fig. 2, OH plays a vital role in the RO_x ($OH + HO_2 + RO + RO_2$) cycle in photochemical reactions through initially oxidizing VOCs, which subsequently leads to O_3 formation [14]. In general, OH concentrations are much lower in winter compared to summer due to the aggravated OH sink caused by higher concentrations of NO_2 (i.e., the reaction of OH and NO_2) (Supplementary Material Table S5), and the reduced photolysis sources (i.e., photolysis of O_3 and HONO) when solar radiation is weak in winter. Such processes could suppress O_3 formation regardless of the abundance of VOCs. In this study, although the average daytime OH concentration on the winter O_3 episode days ($[0.8 \pm 0.1] \times 10^6$ molecules cm^{-3}) was lower than that on summer O_3 episode days ($[2.0 \pm 0.3] \times 10^6$ molecules cm^{-3}) (Supplementary Material Table S6) [40], the average OH concentration during the peak period still reached $(2.0 \pm 0.1) \times 10^6$ molecules cm^{-3}, which was significantly higher than that found in previous studies [75–77]. This high concentration of OH attracted our attention; therefore, we further explored the radical chemistry associated with OH formation.

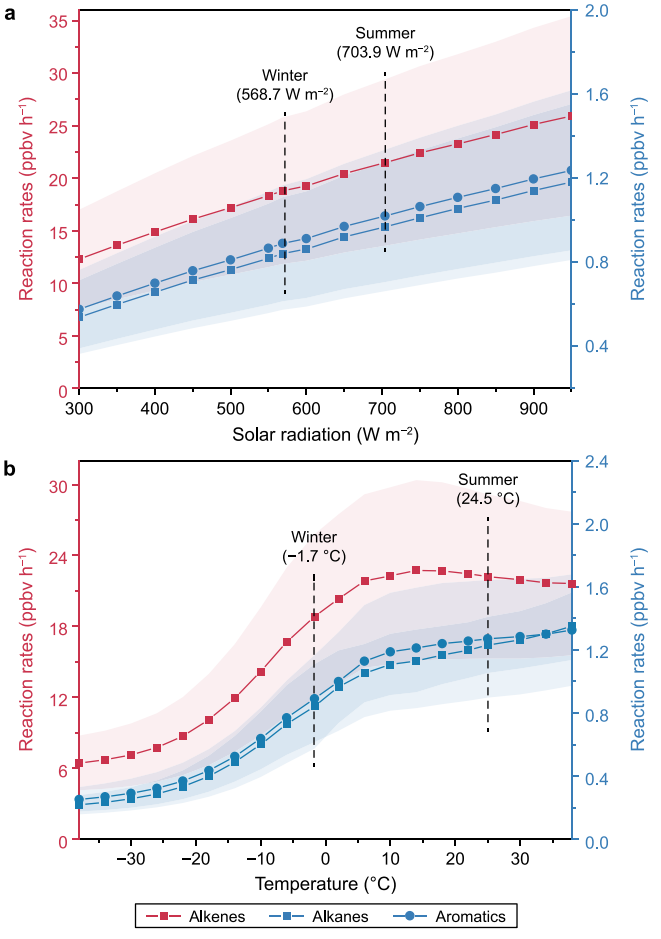

Fig. 1. Reaction rates of VOC groups with OH during the peak period (13:00–16:00 LT) under different solar radiations (**a**) and temperatures (**b**). Black dotted lines represent the daily maximum average solar radiation and daytime average temperature on O_3 episode days in winter and summer, respectively. O_3 episode days in winter include January 1, 13, 16, and 20, 2018.

3.3.1. Sources of OH

Fig. 3a depicts the contributions of initial sources to OH, HO_2, and RO_2 on O_3 episode days. It was found that the ozonolysis of alkenes made an extraordinary contribution to OH formation, accounting for 90.9 ± 17.6% of the OH sources. As the second contributor, photolysis of HONO accounted for 8.7 ± 0.1% of the OH sources, and the remaining sources contributed a total of 0.4 ± 0.1%. Therefore, O_3–alkene reactions were discovered to be the predominant sources of OH. Furthermore, alkene ozonolysis can occur in a dark environment [78,79]. A handful of studies have shown that O_3 + alkenes contribute to OH formation. For example, it was reported that the maximum daily average contribution of O_3 + alkenes to OH was $(0.3 \pm 0.1) \times 10^7$ molecules cm^{-3} s^{-1} in Shanghai in the summer of 2018 [40]. The value at a mountainous background site in South China (Nanling site) was found to be $(0.03 \pm 0.01) \times 10^7$ molecules cm^{-3} s^{-1} [80]. The contribution level reported at both urban and background sites in the literature is significantly lower than the $(2.1 \pm 0.7) \times 10^7$ molecules cm^{-3} s^{-1} determined in this study (Supplementary Material Fig. S15). The reactions involving O_3 + alkenes were neglected in previous work due to their minor contributions to OH formation. To investigate the sources of OH further, we compared the simulated results with and without OH radicals generated by Criegee intermediates (CIs) via model simulations. The results indicated that 31.0 ± 6.3% of the OH was reduced when OH radicals produced by CIs were excluded (Supplementary Material Fig. S16). CIs generated by the ozonolysis

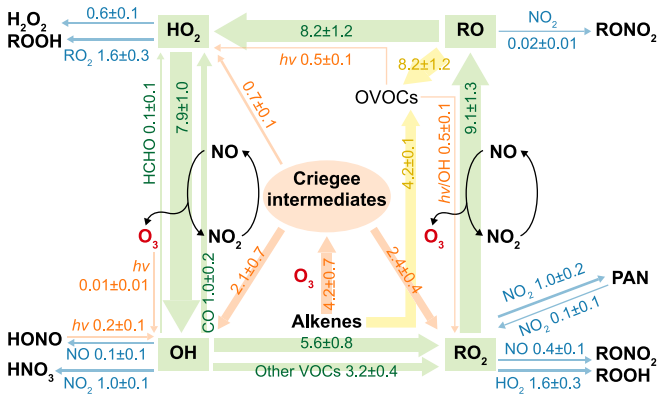

Fig. 2. Daytime (08:00–20:00 LT) average budget of RO_x on O_3 episode days (January 1, 13, 16, and 20, 2018) (unit: $\times 10^7$ molecules cm^{-3} s^{-1}). The orange, blue, and green arrows indicate the initiation, termination, and recycling pathways of radicals, respectively, and the yellow arrows denote reactions related to OVOCs.

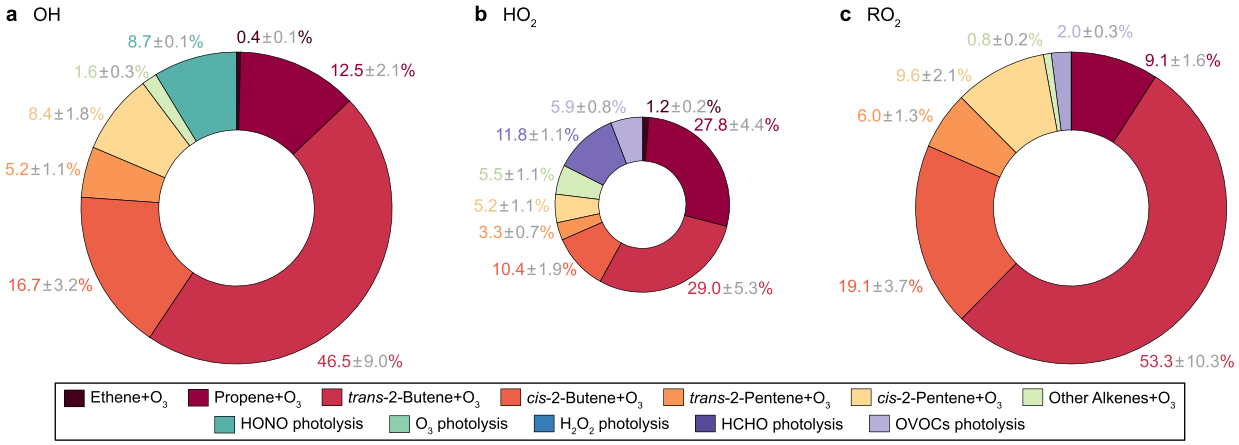

Fig. 3. Daytime (08:00–20:00 LT) average contributions of initial sources to OH (**a**), HO_2 (**b**), and RO_2 (**c**) on O_3 episode days (January 1, 13, 16, and 20, 2018). The size of the ring areas reflects the production rates of OH, HO_2, and RO_2. The contributions of O_3 photolysis and H_2O_2 photolysis to OH formation are omitted (< 0.4%).

of alkenes can rapidly decompose into OH, HO_2, and RO_2 (e.g., *trans*-2-butene, SR1) and were determined to be one of the major sources of radicals in this study [47,81–84]. Specifically, *trans*/*cis*-2-butenes accounted for 63.2 ± 12.2% of OH initiation (Fig. 3a). CH_3CHOOB, a CI species named in MCM, generated from *trans*/*cis*-2-butene/pentene, was the largest contributor to OH, contributing to a daytime average of $(1.6 \pm 0.3) \times 10^7$ molecules cm^{-3} s^{-1} of OH on O_3 episode days (Supplementary Material Table S7). Table S8 (Supplementary Material) compares the average daytime reaction rates between alkenes with OH and alkenes with O_3. It was found that the reaction rates of *trans*/*cis*-2-butene/pentene with O_3 were higher than those with OH. However, the reaction rates of OH with other alkenes, particularly propene, were found to be greater (Supplementary Material Fig. S15b). This indicated that *trans*/*cis*-2-butene/pentenes tended to react with O_3 and thus promote the initiation of OH, which, in turn, enhanced VOC oxidation and participated in radical cycling, ultimately leading to significant O_3 production (Supplementary Material Fig. S15a).

3.3.2. Sources of HO_2 and RO_2

In addition to OH, CIs can be decomposed into HO_2 and RO_2, which also play important roles in radical cycling [81,83–86]. Fig. 3b and c show the predominant initiations of HO_2 and RO_2 on O_3 episode days, respectively. Alkene ozonolysis accounted for 82.4 ± 14.7% and 98.0 ± 19.1% of the initiated HO_2 and RO_2, respectively, which was in sharp contrast to the findings of previous studies that showed the photolysis of OVOCs was the main source of HO_2 and RO_2 [86]. As shown in Fig. 2, HO_2 and RO_2 promoted OH formation by accelerating RO_x cycling, resulting in more VOCs participating in the propagation reactions. A more detailed description of the RO_x cycling can be found in Text S9 (Supplementary Material). Moreover, HO_2 and RO_2 generated by the ozonolysis of alkenes reacted directly with NO, subsequently producing O_3 (Fig. 2). This was different from previous studies, where O_3 formation was mainly achieved through the OH-initiated oxidation of VOCs [40]. The average daytime reaction rates of RO_2 and HO_2 produced from O_3 + alkenes were $(2.4 \pm 0.4) \times 10^7$ and $(0.7 \pm 0.1) \times 10^7$ molecules cm^{-3} s^{-1}, respectively, which were the largest contributors excluding OH + VOCs and RO_2 + NO (Supplementary Material Table S6), suggesting a crucial role for alkene ozonolysis in RO_2 and HO_2 initiations. Furthermore, methylperoxy radical (CH_3O_2) accounted for the vast majority of RO_2 species produced by alkene–O_3 reactions (72.4 ± 14.0%); it was mainly generated from *trans*/*cis*-2-butene/pentenes (Supplementary Material Table S7). Therefore, the abovementioned peroxy radicals boosted the production of O_3 by directly reacting with NO and accelerating the RO_x cycling. Overall, despite the lower temperatures and weaker solar radiation levels in winter, a large amount of alkenes emitted from the local petrochemical industry could still enter the radical cycling by reacting with O_3. Alkene ozonolysis dominated the massive O_3 production by generating OH, which subsequently promoted the oxidation of VOCs and formed RO_2 and HO_2, accelerating RO_x cycling and directly producing O_3 via reactions with NO.

3.4. Quantification of O_3 formation

3.4.1. O_3 production and destruction

Fig. 4a shows the average diurnal profiles of simulated O_3 production and destruction rates on O_3 episode days in winter, compared to those on O_3 non-episode days in winter and summer (Supplementary Material Table S9). The average daytime net O_3 production rate was significantly higher on O_3 episode days in winter (17.0 ± 2.3 ppbv h^{-1}) compared to that in summer (8.9 ± 1.7 ppbv h^{-1}) ($p > 0.05$) [40]. Meanwhile, the maximum O_3 production rate (53.4 ppbv h^{-1}) during winter O_3 episode days was greater than that during summer O_3 episode days (~21 ppbv h^{-1}) [40]. In addition, we found that compared to other Chinese cities in summer, O_3 production was more intensive in Lanzhou, which was considered more conducive to O_3 formation. The rates recorded in other cities include 4.6–7.0 ppbv h^{-1} (Wuhan), 3.4–4.6 ppbv h^{-1} (Chengdu), 5.1–7.7 ppbv h^{-1} (Beijing), and 2.1–3.5 ppbv h^{-1} (Shanghai) [40].

The HO_2 + NO and RO_2 + NO pathways dominated O_3 production. Specifically, 90.8 ± 8.5% and 88.4 ± 9.7% of the two respective pathways were related to alkenes via the donation of peroxy radicals. The contributions of alkene species to the HO_2 + NO and RO_2 + NO pathways were quantified in Section 3.4.2. Furthermore, 78.0 ± 11.5% of O_3 destruction resulted from the reactions of alkenes with O_3, which was different from the main reaction of NO_2 with OH in Lanzhou during summer and in other regions in China [40]. Although O_3 was destructed by reactions with alkenes, the radicals generated from these pathways produced more than twice the amount of O_3 through radical initiation compared to the O_3 loss, especially for the butene isomers (Fig. 4b). These findings showed that the reactions of alkenes with O_3 governed O_3 production and destruction and thus further indicated the pivotal role that alkenes play in O_3 pollution.

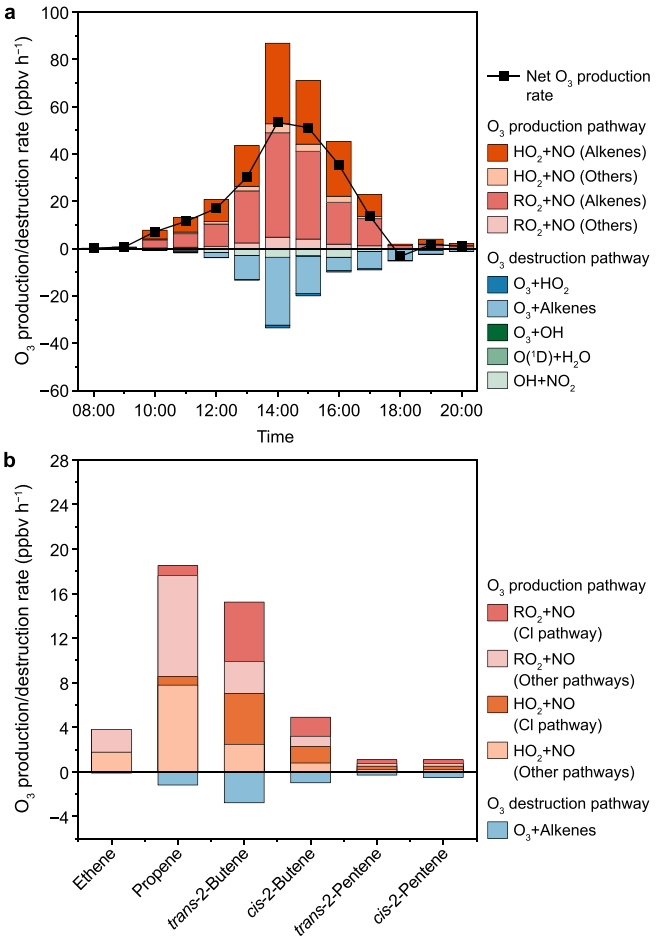

Fig. 4. **a**, Daytime (08:00–20:00 LT) average profiles of simulated O_3 production and destruction rates of main pathways on O_3 episode days. **b**, Daytime average pathway contributions of major alkenes to O_3 production and destruction rates on O_3 episode days. O_3 episode days include January 1, 13, 16, and 20, 2018.

3.4.2. Contributions of alkenes to O_3 production

Fig. 5 presents the detailed evolution of major alkene species and their contributions to O_3 production during the peak period (13:00–16:00 LT) on O_3 episode days. The O_3 production was dominated by the RO_2 + NO and HO_2 + NO pathways (Fig. 4a), responsible for 54.3 ± 5.0% and 45.6 ± 4.0%, respectively.

When we analyzed the origin of RO_2 in the RO_2 + NO pathway, three radicals were found to account for most of the reactions with NO: 1-hydroxypropane-2-ylperoxy radical ($HYPROPO_2$), CH_3O_2, and 3-hydroxy-2-butylperoxy radical ($BUT2OLO_2$). These radicals explained 30.9 ± 2.9%, 27.9 ± 3.8%, and 11.5 ± 1.7% of the RO_2 + NO pathway, respectively. $HYPROPO_2$ and $BUT2OLO_2$ were mainly generated by the OH-initiated oxidation of propene and *trans*/*cis*-2-butene, respectively (Fig. 5). In addition, 2-hydroxyethylperoxy radical ($HOCH_2CH_2O_2$) and 3-hydroxy-2-pentylperoxy radicals ($PE2ENEAO_2$ and $PE2ENEBO_2$) originated from the OH-initiated oxidation of ethene and *trans*/*cis*-2-pentene, responsible for 6.5 ± 0.7% and 1.5 ± 0.3% of RO_2 in the RO_2 + NO pathway, respectively. Unlike the abovementioned radicals, CH_3O_2 was mainly produced by the ozonolysis of alkenes, and 87.8 ± 16.5% of it was derived from CH_3CHOOB, which was one of the CIs. More specifically, 91.8 ± 18.5% of CH_3CHOOB was produced by the ozonolysis of *trans*/*cis*-2-butene, and the remainder was generated by the ozonolysis of propene (8.2 ± 2.7%). Additionally, 10.7 ± 1.4% of CH_3O_2 evolved from CH_3CHOOA, another CI produced by the ozonolysis of propene. Finally, 1.0 ± 0.1% of RO_2 in the RO_2 + NO pathway was ethylperoxy radical ($C_2H_5O_2$), which was derived from a CI (C_2H_5CHOOB) produced by the ozonolysis of *trans*/*cis*-2-pentene.

Regarding the HO_2 + NO pathway, HO_2 was found to be derived from alkyl peroxy radicals, which followed the evolution of RO_2 → RO → HO_2. Thus, the sources of HO_2 in the HO_2 + NO pathway were similar to those of RO_2 in the RO_2 + NO pathway. Specifically, radicals including 1-hydroxypropane-2-yloxy radical (HYPROPO), methoxy radical (CH_3O), 3-hydroxy-2-butyloxy radical (BUT2OAO), and 2-hydroxyethoxy radical ($HOCH_2CH_2O$) provided 31.2 ± 3.5%, 27.8 ± 4.6%, 11.2 ± 2.0%, and 6.6 ± 1.4% of HO_2, respectively, in this pathway. The RO from remaining alkenes contributed 6.0 ± 1.4% of HO_2. In addition, formaldehyde (HCHO) generated from HYPROPO and CH_3O radicals contributed 2.4 ± 0.3% of HO_2 in the HO_2 + NO pathway. Furthermore, a small HO_2 contribution (2.9 ± 0.4%) was provided by C_1–C_3 aldehydes produced from either alkenes or their alkyl radicals.

Overall, 89.6 ± 8.7% of O_3 production on the O_3 episode days was attributed to alkenes. The four largest contributors were *trans*/*cis*-2-butene (34.8 ± 3.7% of the total O_3 production), propene (34.5 ± 5.3%), ethene (6.6 ± 0.8%), and *trans*/*cis*-2-pentene (4.7 ± 0.9%). Other VOC groups only contributed 10.4 ± 9.5% of O_3 production.

Given the dominant role that alkenes were found to play in O_3 production, we evaluated a series of O_3 control strategies related to alkenes, as shown in Fig. S18a (Supplementary Material). It was found that a reduction of approximately 84.2% propene or 80.7% *trans*/*cis*-2-butene could prevent the hourly maximum O_3 concentration from exceeding 100 ppbv. However, mitigation strategies were found to be less effective for other single alkene species. As discussed in Section 3.4.2, butene isomers and propene were the two most important sources of O_3 production. Notably, if total alkenes were reduced by 26.4%, the hourly maximum O_3 concentration would be lower than 100 ppbv (Supplementary Material Fig. S18b) due to the combined effect of butene isomers and propene. Moreover, if the reduction was solely performed in the early afternoon (i.e., 28.6% reduction in alkenes between 13:00 and 16:00 LT), excessive O_3 concentrations (> 100 ppbv) could be prevented (Supplementary Material Fig. S18b).

3.5. Impact of NO_x

Despite the considerable influence of alkenes, the impact of NO_x cannot be ignored. The NO concentration increased from 17:00 to 21:00 LT and remained relatively high until 10:00 LT the next day, resulting in the nighttime O_3 concentration being close to zero due to the NO titration effect (Supplementary Material Fig. S12a). Subsequently, it hindered the ozonolysis of alkenes after 17:00 LT and before 10:00 LT (Supplementary Material Fig. S19c). In addition, RIR values were calculated to determine the relationship between O_3 and its precursors. Overall, the average daytime RIR values of NO_x were negative, suggesting an inhibitory effect on O_3 formation (Supplementary Material Fig. S20a). Specifically, the negative hourly RIR values of NO_x were mainly concentrated in the mornings and evenings (Supplementary Material Fig. S20b). This was attributed to the NO titration effect, which inhibited the ozonolysis of alkenes and subsequently restricted the reactions of HO_2 and RO_2 with NO. However, the hourly RIR values of NO_x were positive from 12:00 to 17:00 LT (Supplementary Material Fig. S20b), indicating that O_3 formation was co-limited by VOCs and NO_x during this period, consistent with that in summer [40]. After sunrise, as NO_2 photolysis increased, more O_3 was produced and participated in reactions with alkenes (Supplementary Material Fig. S19c). Furthermore, the RIR values of NO_x were higher than

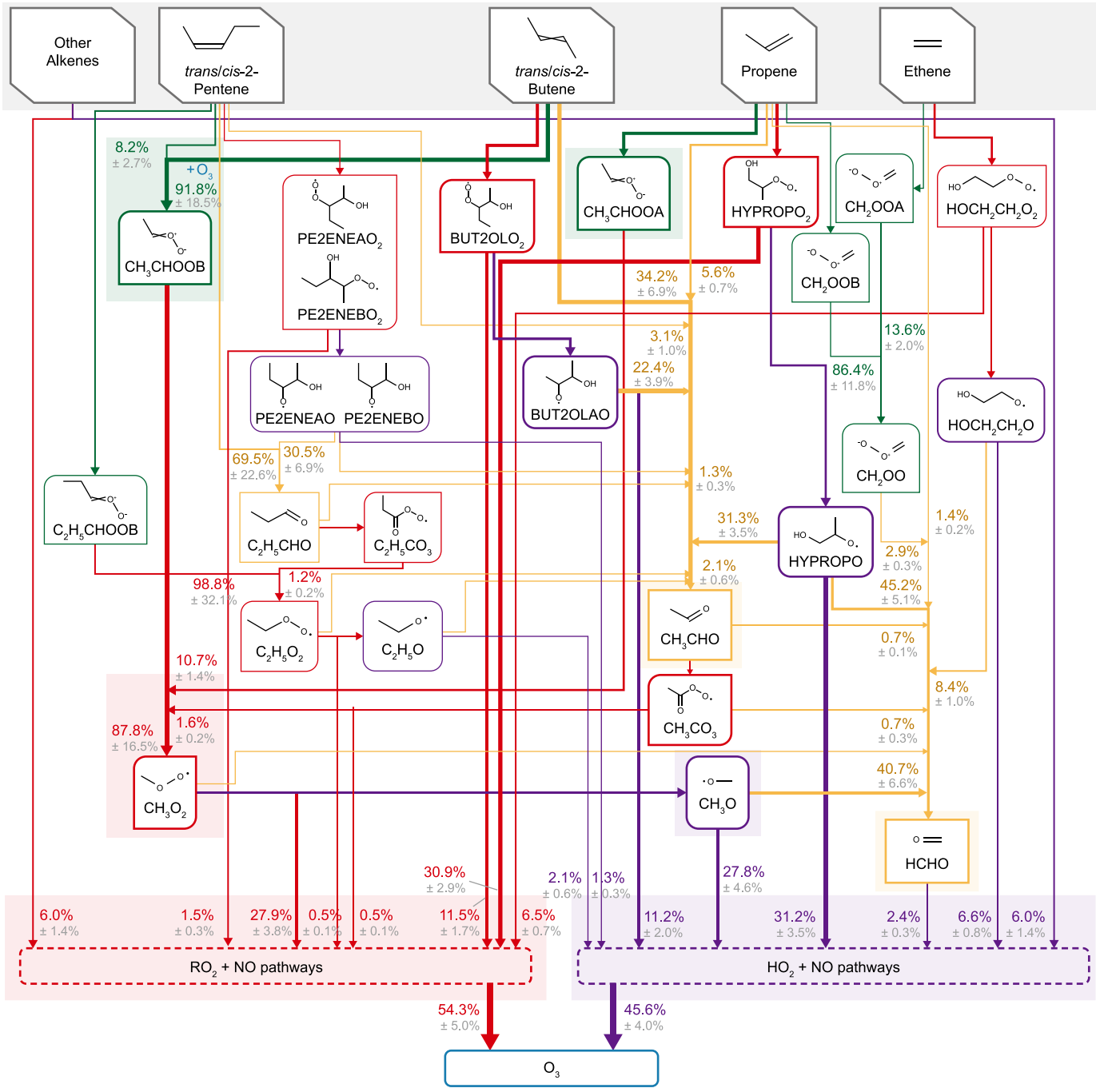

Fig. 5. Evolution processes of alkenes and their contributions to O_3 formation during the peak period (13:00–16:00 LT) on O_3 episode days (January 1, 13, 16, and 20, 2018).

those of alkenes from 14:00 to 17:00 LT (Supplementary Material Fig. S20b), implying that O_3 formation inclined into a NO_x-limited regime. Therefore, it was found that a 27.7% reduction in NO_x during the period of 13:00–16:00 LT could effectively maintain the O_3 concentration below 100 ppbv (Supplementary Material Fig. S18a).

4. Implications

Contrary to the consensus that O_3 pollution mainly occurs in warm weather with strong solar radiation, we discovered through intensive sampling that O_3 concentrations in Lanzhou were extremely high in winter. Using observation-based box model simulations, we found that large amounts of alkenes emitted from the local petrochemical industry reacted with O_3 and produced Criegee intermediates, which further decomposed into substantial amounts of RO_x and ultimately accelerated O_3 production. *Trans*/*cis*-2-butene, propene, ethene, and *trans*/*cis*-2-pentene were identified as the top four alkenes, accounting for more than 80% of O_3 production. We also discovered that temperature changes had a limited impact on the ozonolysis of alkenes, which can also occur in dark environments. Our findings provide new information that challenges the consensus, showing that warm weather and strong solar radiation are not indispensable factors for intensive photochemical reactions and that dark reactions in photochemistry could

surpass photolysis reactions and trigger intense O_3 production. Moreover, our findings challenge the understanding that alkene ozonolysis mainly leads to the destruction of O_3; in this study, it was the culprit responsible for severe O_3 pollution. Given the increased industrialization and elevated demand for olefin products worldwide, paying serious attention to alkene-related air pollution is essential. Furthermore, high snow albedo could intensify the RO_x cycling and O_3 production processes identified in this study. The findings of this study emphasize the importance of recognizing O_3 pollution in locations with cold weather and weak sunlight and provide a reference for studying atmospheric oxidation reactions and radical chemistry in petrochemical industrial environments. The control measures proposed in this study are also applicable to similar regions.

CRediT authorship contribution statement

Jin Yang: Writing - Original Draft, Methodology, Formal Analysis, Visualization, Validation, Software. **Yangzong Zeren:** Writing - Original Draft, Methodology, Investigation, Formal Analysis. **Hai Guo:** Writing - Review & Editing, Supervision, Resources, Project Administration, Investigation, Funding Aacquisition, Data Curation, Conceptualization. **Yu Wang:** Writing - Review & Editing, Supervision, Software, Investigation, Formal Analysis, Conceptualization. **Xiaopu Lyu:** Writing - Review & Editing, Validation, Investigation, Formal Analysis. **Beining Zhou:** Visualization, Validation, Software, Formal Analysis. **Hong Gao:** Writing - Review & Editing, Resources, Data Curation. **Dawen Yao:** Formal Analysis, Investigation, Validation. **Zhanxiang Wang:** Investigation, Formal Analysis. **Shizhen Zhao:** Methodology, Investigation. **Jun Li:** Writing - Review & Editing, Validation, Investigation. **Gan Zhang:** Writing - Review & Editing, Investigation, Data Curation.

Declaration of competing interest

The authors declare that they have no known competing financial interests or personal relationships that could have appeared to influence the work reported in this paper.

Acknowledgments

This work was supported by the Research Grants Council (RGC) of the Government of the Hong Kong Special Administrative Region (PolyU 152124/21 E and N_PolyU530/20), the research support scheme of Research Institute for Land and Space at The Hong Kong Polytechnic University (1-CD79), and the Start-up Fund for RAPs under the Strategic Hiring Scheme of the Hong Kong Polytechnic University (1-BD3T). We thank Lanzhou University for providing the data.

Appendix A. Supplementary data

Supplementary data to this article can be found online at https://doi.org/10.1016/j.ese.2024.100477.

References

[1] W.L. Chameides, H. Yu, S.C. Liu, M. Bergin, X. Zhou, L. Mearns, G. Wang, C.S. Kiang, R.D. Saylor, C. Luo, Y. Huang, A. Steiner, F. Giorgi, Case study of the effects of atmospheric aerosols and regional haze on agriculture: an opportunity to enhance crop yields in China through emission controls? P Natl Acad Sci USA 96 (24) (1999) 13626–13633.
[2] M.R. Ashmore, Assessing the future global impacts of ozone on vegetation, Plant Cell Environ. 28 (8) (2005) 949–964.
[3] X. Wang, W. Manning, Z. Feng, Y. Zhu, Ground-level ozone in China: distribution and effects on crop yields, Environ. Pollut. 147 (2) (2007) 394–400.
[4] D. Simpson, A. Arneth, G. Mills, S. Solberg, J. Uddling, Ozone — the persistent menace: interactions with the N cycle and climate change, Curr. Opin. Environ. Sustain. 9–10 (2014) 9–19.
[5] E.A. Ainsworth, C.R. Yendrek, S. Sitch, W.J. Collins, L.D. Emberson, The effects of tropospheric ozone on net primary productivity and implications for climate change, Annu. Rev. Plant Biol. 63 (2012) 637–661.
[6] A.L. Jennifer, Tropospheric ozone: seasonal behavior, trends, and anthropogenic influence, J. Geophys. Res. Atmos. 90 (1985) 10463–10482.
[7] W.J. Collins, Effect of stratosphere-troposphere exchange on the future tropospheric ozone trend, J. Geophys. Res. 108 (D12) (2003).
[8] J.N. Cape, Surface ozone concentrations and ecosystem health: past trends and a guide to future projections, Sci. Total Environ. 400 (1–3) (2008) 257–269.
[9] X. Lu, L. Zhang, L. Shen, Meteorology and climate influences on tropospheric ozone: a review of natural sources, chemistry, and transport patterns, Current Pollution Reports 5 (4) (2019) 238–260.
[10] H. Guo, F. Jiang, H.R. Cheng, I.J. Simpson, X.M. Wang, A.J. Ding, T.J. Wang, S.M. Saunders, T. Wang, S.H.M. Lam, D.R. Blake, Y.L. Zhang, M. Xie, Concurrent observations of air pollutants at two sites in the Pearl River Delta and the implication of regional transport, Atmos. Chem. Phys. 9 (19) (2009) 7343–7360.
[11] H. Guo, Z.H. Ling, K. Cheung, F. Jiang, D.W. Wang, I.J. Simpson, B. Barletta, S. Meinardi, T.J. Wang, X.M. Wang, S.M. Saunders, D.R. Blake, Characterization of photochemical pollution at different elevations in mountainous areas in Hong Kong, Atmos. Chem. Phys. 13 (8) (2013) 3881–3898.
[12] Y.J. Li, B.P. Lee, L. Su, J.C.H. Fung, C.K. Chan, Seasonal characteristics of fine particulate matter (PM) based on high-resolution time-of-flight aerosol mass spectrometric (HR-ToF-AMS) measurements at the HKUST Supersite in Hong Kong, Atmos. Chem. Phys. 15 (1) (2015) 37–53.
[13] L. Li, J.Y. An, Y.Y. Shi, M. Zhou, R.S. Yan, C. Huang, H.L. Wang, S.R. Lou, Q. Wang, Q. Lu, J. Wu, Source apportionment of surface ozone in the Yangtze River Delta, China in the summer of 2013, Atmos. Environ. 144 (2016) 194–207.
[14] T. Wang, L.K. Xue, P. Brimblecombe, Y.F. Lam, L. Li, L. Zhang, Ozone pollution in China: a review of concentrations, meteorological influences, chemical precursors, and effects, Sci. Total Environ. 575 (2017) 1582–1596.
[15] Y. Wang, H. Wang, H. Guo, X.P. Lyu, H.R. Cheng, Z.H. Ling, P.K.K. Louie, I.J. Simpson, S. Meinardi, D.R. Blake, Long-term O-3-precursor relationships in Hong Kong: field observation and model simulation, Atmos. Chem. Phys. 17 (18) (2017) 10919–10935.
[16] X. Lu, L. Zhang, X.L. Wang, M. Gao, K. Li, Y.Z. Zhang, X. Yue, Y.H. Zhang, Rapid increases in warm-season surface ozone and resulting health impact in China since 2013, Environ. Sci. Technol. Lett. 7 (4) (2020) 240–247.
[17] S.J.a.L.I. Oltmans, Hiram. Surface ozone measurements from a global network, Atmos. Environ. 28 (1) (1994) 9–24.
[18] N.A.S. Kgabi, M. Ramotsamai, Seasonal variations of tropospheric ozone concentrations, Global journal of science frontier research chemistry 12 (2012) 21–29.
[19] N. Liu, W. Lin, J. Ma, W. Xu, X. Xu, Seasonal variation in surface ozone and its regional characteristics at global atmosphere watch stations in China, J. Environ. Sci. (China) 77 (2019) 291–302.
[20] K.J. Maji, W.F. Ye, M. Arora, S.M.S. Nagendra, Ozone pollution in Chinese cities: assessment of seasonal variation, health effects and economic burden, Environ. Pollut. 247 (2019) 792–801.
[21] A. Singh, S.M. Sarin, P. Shanmugam, N. Sharma, A.K. Attri, V.K. Jain, Ozone distribution in the urban environment of Delhi during winter months, Atmospheric Environment, Atmos. Environ. 31 (20) (1997) 3421–3427.
[22] R.C. Schnell, S.J. Oltmans, R.R. Neely, M.S. Endres, J.V. Molenar, A.B. White, Rapid photochemical production of ozone at high concentrations in a rural site during winter, Nat. Geosci. 2 (2) (2009) 120–122.
[23] S. Oltmans, R. Schnell, B. Johnson, G. Pétron, T. Mefford, R. Neely, D. Helmig, G. Pfister, Anatomy of wintertime ozone associated with oil and natural gas extraction activity in Wyoming and Utah, Elementa: Science of the Anthropocene 2 (2014).
[24] P.M. Edwards, S.S. Brown, J.M. Roberts, R. Ahmadov, R.M. Banta, J.A. deGouw, W.P. Dube, R.A. Field, J.H. Flynn, J.B. Gilman, M. Graus, D. Helmig, A. Koss, A.O. Langford, B.L. Lefer, B.M. Lerner, R. Li, S.M. Li, S.A. McKeen, S.M. Murphy, D.D. Parrish, C.J. Senff, J. Soltis, J. Stutz, C. Sweeney, C.R. Thompson, M.K. Trainer, C. Tsai, P.R. Veres, R.A. Washenfelder, C. Warneke, R.J. Wild, C.J. Young, B. Yuan, R. Zamora, High winter ozone pollution from carbonyl photolysis in an oil and gas basin, Nature 514 (7522) (2014) 351–354.
[25] K. Li, D.J. Jacob, H. Liao, Y. Qiu, L. Shen, S. Zhai, K.H. Bates, M.P. Sulprizio, S. Song, X. Lu, Q. Zhang, B. Zheng, Y. Zhang, J. Zhang, H.C. Lee, S.K. Kuk, Ozone pollution in the North China Plain spreading into the late-winter haze season, Proc. Natl. Acad. Sci. U. S. A. 118 (10) (2021).
[26] L. Ma, F. Fu, Z. Li, P. Liu, Oil development in China: current status and future trends, Energy Pol. 45 (2012) 43–53.
[27] S.Y. Chen, Q. Zhang, B. McLellan, T.T. Zhang, Review on the petroleum market in China: history, challenges and prospects, Petrol. Sci. 17 (6) (2020) 1779–1794.
[28] T. Chen, L. Xue, P. Zheng, Y. Zhang, Y. Liu, J. Sun, G. Han, H. Li, X. Zhang, Y. Li, H. Li, C. Dong, F. Xu, Q. Zhang, W. Wang, Volatile organic compounds and ozone air pollution in an oil production region in northern China, Atmos. Chem. Phys. 20 (11) (2020) 7069–7086.
[29] J. Zhan, W. Ma, B. Song, Z. Wang, X. Bao, H.B. Xie, B. Chu, H. He, T. Jiang, Y. Liu, The contribution of industrial emissions to ozone pollution: identified using ozone formation path tracing approach, NPJ Clim Atmos Sci 6 (1) (2023) 37.
[30] X.Y. Tang, B.S. Tian, C.H. Chen, Z.H. Reng, A study of photochemical smog

pollution and its control at the Xigu district in Lanzhou city, Chin. J. Environ. Sci. 5 (1985) 1–11.
[31] X.F. Li, Q.H. Zhang, H.W. Xue, The role of initial cloud condensation nuclei concentration in hail using the WRF NSSL 2-moment microphysics scheme, Adv. Atmos. Sci. 34 (9) (2017) 1106–1120.
[32] W. Guo, Q. Chen, Y. Yang, Y. Zhang, X. Liu, R. Zhang, Y. Zhu, G. Li, P. Liu, M. Chen, Investigating the mechanism of morning ozone concentration peaks in a petrochemical industrial city, Atmos. Environ. 270 (2022).
[33] J. Liu, Y. Ruan, Q. Wu, Y. Ma, X. He, L. Li, S. Li, J. Niu, B. Luo, Has the mortality risk declined after the improvement of air quality in an ex-heavily polluted Chinese city-Lanzhou? Chemosphere 242 (2020) 125196.
[34] G.Y. Wang, S.M. Jia, R.H. Li, S.R. Ma, X.F. Chen, Z.J. Wu, G.F. Shi, X.L. Niu, Seasonal variation characteristics of hydroxyl radical pollution and its potential formation mechanism during the daytime in Lanzhou, J. Environ. Sci. 95 (2020) 58–64.
[35] J. Dong, Y. Liu, H. Bao, Revalue associations of short-term exposure to air pollution with respiratory hospital admissions in Lanzhou, China after the control and treatment of current pollution, Int. J. Hyg Environ. Health 231 (2021) 113658.
[36] C. Yan, L. Wang, Q. Zhang, Study on coupled relationship between urban air quality and Land use in Lanzhou, China, Sustainability-Basel 13 (14) (2021).
[37] C. Jia, X. Mao, T. Huang, X. Liang, Y. Wang, Y. Shen, W. Jiang, H. Wang, Z. Bai, M. Ma, Z. Yu, J. Ma, H. Gao, Non-methane hydrocarbons (NMHCs) and their contribution to ozone formation potential in a petrochemical industrialized city, Northwest China, Atmos. Res. 169 (2016) 225–236.
[38] W. Guo, Y. Yang, Q. Chen, Y. Zhu, Y. Zhang, Y. Zhang, Y. Liu, G. Li, W. Sun, J. She, Chemical reactivity of volatile organic compounds and their effects on ozone formation in a petrochemical industrial area of Lanzhou, Western China, Sci. Total Environ. 839 (2022) 155901.
[39] L.K. Xue, T. Wang, J. Gao, A.J. Ding, X.H. Zhou, D.R. Blake, X.F. Wang, S.M. Saunders, S.J. Fan, H.C. Zuo, Q.Z. Zhang, W.X. Wang, Ground-level ozone in four Chinese cities: precursors, regional transport and heterogeneous processes, Atmos. Chem. Phys. 14 (23) (2014) 13175–13188.
[40] X.F. Liu, H. Guo, L.W. Zeng, X. Lyu, Y. Wang, Y.Z. Zeren, J. Yang, L.Y. Zhang, S.Z. Zhao, J. Li, G. Zhang, Photochemical ozone pollution in five Chinese megacities in summer 2018, Sci. Total Environ. 801 (2021).
[41] B.H. Henderson, H.E. Jeffries, B.U. Kim, W.G. Vizuete, The influence of model resolution on ozone in industrial volatile organic compound plumes, J. Air Waste Manag. Assoc. 60 (9) (2010) 1105–1117.
[42] M.E.a.S. Jenkin, M. Sandra, Michael J. Pilling, The tropospheric degradation of volatile organic compounds: a protocol for mechanism development, Atmos. Environ. 31 (1) (1997) 81–104.
[43] M.E. Jenkin, S.M. Saunders, V. Wagner, M.J. Pilling, Protocol for the development of the Master Chemical Mechanism, MCM v3 (Part B): tropospheric degradation of aromatic volatile organic compounds, Atmos. Chem. Phys. 3 (1) (2003) 181–193.
[44] S.M. Saunders, M.E. Jenkin, R.G. Derwent, M.J. Pilling, Protocol for the development of the Master Chemical Mechanism, MCM v3 (Part A): tropospheric degradation of non-aromatic volatile organic compounds, Atmos. Chem. Phys. 3 (1) (2003) 161–180.
[45] S.H.M. Lam, S.M. Saunders, H. Guo, Z.H. Ling, F. Jiang, X.M. Wang, T.J. Wang, Modelling VOC source impacts on high ozone episode days observed at a mountain summit in Hong Kong under the influence of mountain-valley breezes, Atmos. Environ. 81 (2013) 166–176.
[46] X.P. Lyu, N. Chen, H. Guo, W.H. Zhang, N. Wang, Y. Wang, M. Liu, Ambient volatile organic compounds and their effect on ozone production in Wuhan, central China, Sci. Total Environ. 541 (2016) 200–209.
[47] Y. Wang, H. Guo, S.C. Zou, X.P. Lyu, Z.H. Ling, H.R. Cheng, Y.Z. Zeren, Surface O-3 photochemistry over the South China Sea: application of a near-explicit chemical mechanism box model, Environ. Pollut. 234 (2018) 155–166.
[48] X.P. Lyu, N. Wang, H. Guo, L.K. Xue, F. Jiang, Y.Z. Zeren, H.R. Cheng, Z. Cai, L.H. Han, Y. Zhou, Causes of a continuous summertime O-3 pollution event in Jinan, a central city in the North China Plain, Atmos. Chem. Phys. 19 (5) (2019) 3025–3042.
[49] X.F. Liu, X.P. Lyu, Y. Wang, F. Jiang, H. Guo, Intercomparison of O-3 formation and radical chemistry in the past decade at a suburban site in Hong Kong, Atmos. Chem. Phys. 19 (7) (2019) 5127–5145.
[50] N. Wang, Z.H. Ling, X.J. Deng, T. Deng, X.P. Lyu, T.Y. Li, X.R. Gao, X. Chen, Source contributions to PM2.5 under unfavorable weather conditions in guangzhou city, China, Adv. Atmos. Sci. 35 (9) (2018) 1145–1159.
[51] W. Zhang, S. Tong, M. Ge, J. An, Z. Shi, S. Hou, K. Xia, Y. Qu, H. Zhang, B. Chu, Y. Sun, H. He, Variations and sources of nitrous acid (HONO) during a severe pollution episode in Beijing in winter 2016, Sci. Total Environ. 648 (2019) 253–262.
[52] W. Li, S. Tong, J. Cao, H. Su, W. Zhang, L. Wang, C. Jia, X. Zhang, Z. Wang, M. Chen, M. Ge, Comparative observation of atmospheric nitrous acid (HONO) in Xi'an and Xianyang located in the GuanZhong basin of western China, Environ. Pollut. 289 (2021) 117679.
[53] X. Zhang, S. Tong, C. Jia, W. Zhang, J. Li, W. Wang, Y. Sun, X. Wang, L. Wang, D. Ji, L. Wang, P. Zhao, G. Tang, J. Xin, A. Li, M. Ge, The levels and sources of nitrous acid (HONO) in winter of Beijing and sanmenxia, J. Geophys. Res. Atmos. 127 (10) (2022).
[54] C.A. Cardelino, W.L. Chameides, An observation-based model for analyzing ozone precursor relationships in the urban atmosphere, J. Air Waste Manag. Assoc. 45 (3) (1995) 161–180.
[55] L.K. Xue, T. Wang, P.K.K. Louie, C.W.Y. Luk, D.R. Blake, Z. Xu, Increasing external effects negate local efforts to control ozone air pollution: a case study of Hong Kong and implications for other Chinese cities, Environ. Sci. Technol. 48 (18) (2014) 10769–10775.
[56] L. Liu, X. Ma, W. Wen, C. Sun, J. Jiao, Characteristics and potential sources of wintertime air pollution in Linfen, China, Environ. Monit. Assess. 193 (5) (2021) 252.
[57] L. Shen, Y. Diao, T. Zhao, X. Gu, S.S. Shi, Meteorological influence on persistent O3 pollution events in wuxi in the yangtze River Delta, China, Sci. Total Environ. 917 (2024) 170484.
[58] J. Yin, C.Y. Gao, J. Hong, Z. Gao, Y. Li, X. Li, S. Fan, B. Zhu, Surface meteorological conditions and boundary layer height variations during an air pollution episode in nanjing, China, J. Geophys. Res. Atmos. 124 (6) (2019) 3350–3364.
[59] M. Gao, G.R. Carmichael, P.E. Saide, Z. Lu, M. Yu, D.G. Streets, Z. Wang, Response of winter fine particulate matter concentrations to emission and meteorology changes in North China, Atmos. Chem. Phys. 16 (18) (2016) 11837–11851.
[60] R. Li, L. Cui, J. Li, A. Zhao, H. Fu, Y. Wu, L. Zhang, L. Kong, J. Chen, Spatial and temporal variation of particulate matter and gaseous pollutants in China during 2014–2016, Atmos. Environ. 161 (2017) 235–246.
[61] B. Chu, Q. Ma, J. Liu, J. Ma, P. Zhang, T. Chen, Q. Feng, C. Wang, N. Yang, H. Ma, J. Ma, A.G. Russell, H. He, Air pollutant correlations in China: secondary air pollutant responses to NOx and SO2 control, Environ. Sci. Technol. Lett. 7 (10) (2020) 695–700.
[62] X. Fu, T. Wang, J. Gao, P. Wang, Y. Liu, S. Wang, B. Zhao, L. Xue, Persistent heavy winter nitrate pollution driven by increased photochemical oxidants in northern China, Environ. Sci. Technol. 54 (7) (2020) 3881–3889.
[63] J. Duan, J. Tan, L. Yang, S. Wu, J. Hao, Concentration, sources and ozone formation potential of volatile organic compounds (VOCs) during ozone episode in Beijing, Atmos. Res. 88 (1) (2008) 25–35.
[64] S.E. Pusede, A.L. Steiner, R.C. Cohen, Temperature and recent trends in the chemistry of continental surface ozone, Chem. Rev. 115 (10) (2015) 3898–3918.
[65] B.D. Belan, D.E. Savkin, The role of air humidity in variations in near-surface ozone concentration, Atmospheric and Oceanic Optics 32 (5) (2019) 586–589.
[66] M. Li, S. Yu, X. Chen, Z. Li, Y. Zhang, L. Wang, W. Liu, P. Li, E. Lichtfouse, D. Rosenfeld, J.H. Seinfeld, Large scale control of surface ozone by relative humidity observed during warm seasons in China, Environ. Chem. Lett. 19 (6) (2021) 3981–3989.
[67] D.H. Tsai, J.L. Wang, C.H. Wang, C.C. Chan, A study of ground-level ozone pollution, ozone precursors and subtropical meteorological conditions in central Taiwan, J. Environ. Monit. 10 (1) (2008) 109–118.
[68] L.R. Hui, X.G. Liu, Q.W. Tan, M. Feng, J.L. An, Y. Qu, Y.H. Zhang, M.Q. Jiang, Characteristics, source apportionment and contribution of VOCs to ozone formation in Wuhan, Central China, Atmos. Environ. 192 (2018) 55–71.
[69] J. Sun, Z. Shen, Y. Zhang, W. Dai, K. He, H. Xu, Z. Zhang, L. Cui, X. Li, Y. Huang, J. Cao, Profiles and source apportionment of nonmethane volatile organic compounds in winter and summer in xi'an, China, based on the hybrid environmental receptor model, Adv. Atmos. Sci. 38 (1) (2020) 116–131.
[70] J.H. Li, S.X. Deng, A. Tohti, G.H. Li, X.X. Yi, Z.Z. Lu, J.Y. Liu, S. Zhang, Spatial characteristics of VOCs and their ozone and secondary organic aerosol formation potentials in autumn and winter in the Guanzhong Plain, China, Environ. Res. 211 (2022).
[71] Z.B. Wang, J.X. Li, L.W. Liang, Spatio-temporal evolution of ozone pollution and its influencing factors in the Beijing-Tianjin-Hebei Urban Agglomeration, Environ. Pollut. 256 (2020) 113419.
[72] J.B. Gilman, B.M. Lerner, W.C. Kuster, J.A. de Gouw, Source signature of volatile organic compounds from oil and natural gas operations in northeastern Colorado, Environ. Sci. Technol. 47 (3) (2013) 1297–1305.
[73] R.A. Field, J. Soltis, M.C. McCarthy, S. Murphy, D.C. Montague, Influence of oil and gas field operations on spatial and temporal distributions of atmospheric non-methane hydrocarbons and their effect on ozone formation in winter, Atmos. Chem. Phys. 15 (6) (2015) 3527–3542.
[74] H. Zheng, S. Kong, X. Xing, Y. Mao, T. Hu, Y. Ding, G. Li, D. Liu, S. Li, S. Qi, Monitoring of volatile organic compounds (VOCs) from an oil and gas station in northwest China for 1 year, Atmos. Chem. Phys. 18 (7) (2018) 4567–4595.
[75] X. Ma, Z. Tan, K. Lu, X. Yang, Y. Liu, S. Li, X. Li, S. Chen, A. Novelli, C. Cho, L. Zeng, A. Wahner, Y. Zhang, Winter photochemistry in Beijing: Observation and model simulation of OH and HO(2) radicals at an urban site, Sci. Total Environ. 685 (2019) 85–95.
[76] D.E. Heard, High levels of the hydroxyl radical in the winter urban troposphere, Geophys. Res. Lett. 31 (18) (2004).
[77] E.J. Slater, L.K. Whalley, R. Woodward-Massey, C. Ye, J.D. Lee, F. Squires, J.R. Hopkins, R.E. Dunmore, M. Shaw, J.F. Hamilton, A.C. Lewis, L.R. Crilley, L. Kramer, W. Bloss, T. Vu, Y. Sun, W. Xu, S. Yue, L. Ren, W.J.F. Acton, C.N. Hewitt, X. Wang, P. Fu, D.E. Heard, Elevated levels of OH observed in haze events during wintertime in central Beijing, Atmos. Chem. Phys. 20 (23) (2020) 14847–14871.
[78] P.A. Ariya, R. Sander, P.J. Crutzen, Significance of HOx and peroxides production due to alkene ozonolysis during fall and winter: a modeling study, J. Geophys. Res. Atmos. 105 (D14) (2000) 17721–17738.
[79] M.S. Alam, A.R. Rickard, M. Camredon, K.P. Wyche, T. Carr, K.E. Hornsby, P.S. Monks, W.J. Bloss, Radical product yields from the ozonolysis of short chain alkenes under atmospheric boundary layer conditions, J. Phys. Chem. A 117 (47) (2013) 12468–12483.

[80] Y. Wang, T. Liu, D. Gong, H. Wang, H. Guo, M. Liao, S. Deng, H. Cai, B. Wang, Anthropogenic pollutants induce changes in peroxyacetyl nitrate formation intensity and pathways in a mountainous background atmosphere in southern China, Environ. Sci. Technol. 57 (15) (2023) 6253–6262.
[81] S. Hatakeyama, Reactions of criegee intermediates in the gas phase, Res. Chem. Intermed. 20 (1994) 503–524.
[82] D.J. Jacob, Introduction to Atmospheric Chemistry, Princeton university press, 1999.
[83] K.M. Emmerson, N. Carslaw, M.J. Pilling, Urban atmospheric chemistry during the PUMA campaign 2: radical budgets for OH, HO2 and RO2, J. Atmos. Chem. 52 (2) (2005) 165–183.
[84] D.L. Osborn, C.A. Taatjes, The physical chemistry of Criegee intermediates in the gas phase, Int. Rev. Phys. Chem. 34 (3) (2015) 309–360.
[85] Z. Tan, F. Rohrer, K. Lu, X. Ma, B. Bohn, S. Broch, H. Dong, H. Fuchs, G.I. Gkatzelis, A. Hofzumahaus, F. Holland, X. Li, Y. Liu, Y. Liu, A. Novelli, M. Shao, H. Wang, Y. Wu, L. Zeng, M. Hu, A. Kiendler-Scharr, A. Wahner, Y. Zhang, Wintertime photochemistry in Beijing: observations of ROx radical concentrations in the North China Plain during the BEST-ONE campaign, Atmos. Chem. Phys. 18 (16) (2018) 12391–12411.
[86] Z.H. Ling, H. Guo, S.H.M. Lam, S.M. Saunders, T. Wang, Atmospheric photochemical reactivity and ozone production at two sites in Hong Kong: application of a Master Chemical Mechanism-photochemical box model, J. Geophys. Res. Atmos. 119 (17) (2014) 10567–10582.